



ELSEVIER

Available at  
www.ComputerScienceWeb.com  
POWERED BY SCIENCE @ DIRECT®

Pattern Recognition Letters 24 (2003) 2127–2134

---

---

Pattern Recognition  
Letters

---

---

www.elsevier.com/locate/patrec

# A robust two step approach for fingerprint identification

Xuejun Tan \*, Bir Bhanu

*Center for Research in Intelligence Systems, University of California, Riverside, CA 92521, USA*

---

## Abstract

Due to the complex distortions involved in two impressions of the same finger, fingerprint identification is still a challenging problem. In this paper, we propose a two step fingerprint identification approach based on the triplets of minutiae. The features that we use to find the potential corresponding triangles include angles, triangle orientation, triangle direction, maximum side, minutiae density and ridge counts. In the first step, based on the number of corresponding triangles between the query fingerprint and the model database constructed offline, hypotheses are generated. In the second step, called verification, false corresponding triangles are eliminated by applying constraints to the transformation between two potential corresponding triangles. The experimental results on National Institute of Standards and Technology special fingerprint database 4, NIST-4, show that the proposed approach provides a reduction by a factor of 10 for the number of the hypotheses that need to be considered if linear search is used and can achieve a good performance even when a large portion of fingerprints in the database are of poor quality.

© 2003 Elsevier Science B.V. All rights reserved.

*Keywords:* Fingerprint indexing; Fingerprint verification; Hypotheses generation; Triangle features; Triplets of minutiae

---

## 1. Introduction

Fingerprints have been used for personal authentication for a long time. Now, they are not only used by police for law enforcement, but they also find their use in civilian applications, such as access control and financial transactions. In terms of applications, there are two kinds of systems, which use fingerprints for the personal identity: verification and identification. In verification, the input is a query fingerprint and an identity (ID), the system verifies whether the ID is consistent

with the fingerprint. The output of a verification system is an answer of yes or no. In identification, the input is only a query fingerprint, the system tries to answer the question: are there any fingerprints in the database, which resemble the query fingerprint? In this paper, we are dealing with the identification problem.

Fingerprint is formed by a group of curves. The most useful features, which include endpoint and bifurcation, are called minutiae. Fig. 1 shows an example of endpoint and bifurcation in a fingerprint image. People believe that a person can be identified with a high confidence based on the minutiae of a fingerprint.

Generally, the minutiae based fingerprint verification is a kind of point matching algorithm. In order to improve the performance, additional

---

\* Corresponding author.

*E-mail addresses:* xtan@cris.ucr.edu (X. Tan), bhanu@cris.ucr.edu (B. Bhanu).

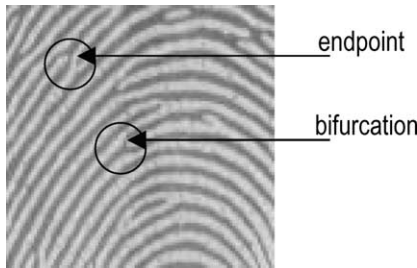


Fig. 1. Examples of minutiae.

characteristics, such as local orientation and core/delta point position are used. However, the distortions between two sets of minutiae extracted from the different impressions of the same finger may include translation, rotation, scale, shear, local perturbation, occlusion and clutter, which make it difficult to find the corresponding minutiae reliably.

There are three kinds of approaches to solve the fingerprint identification problem: (1) repeat the verification procedure for each fingerprint in the database and select the best match; (2) fingerprint classification followed by verification; and (3) fingerprint indexing followed by verification. Fig. 2 shows the block diagram of these three kinds of approaches. The first approach is always based on a verification approach. Recent techniques for fingerprint verification can be found in (Jain et al., 1997; Jiang and Yau, 2000; Kovacs-Vajna, 2000). However, if the size of the database is large, the

first approach will be a time-consuming procedure and it is not practical for real-world applications. The traditional classification techniques used in the fingerprint recognition area attempt to classify fingerprints into five classes: Right loop (R), left loop (L), whorl (W), arch (A) and tented arch (T). Classification techniques based on different features and algorithms can be found in (Cappelli et al., 1999; Jain et al., 1999; Marcialis et al., 2001; Yao et al., 2001). However, the problem of classification technique is that the number of principal classes is small and the fingerprints are unevenly distributed (31.7%, 33.8%, 27.9%, 3.7% and 2.9% for classes R, L, W, A and T, respectively (Wilson et al., 1993)). The classification approach does not narrow down the search enough in the database for efficient identification of a fingerprint. The goal of the third approach is to significantly reduce the number of candidate hypotheses to be considered by the verification algorithm. These approaches are called indexing techniques or 1–N matching in the fingerprint recognition area where the ultimate goal is matching or verification.

A prominent approach for fingerprint identification is by Germain et al. (1997), which integrates the indexing and verification in their approach (Fig. 2(a)). They use the triplets of minutiae in their identification procedure. The features they use are: the length of each side, the angles that the ridges make with respect to the X-axis of the reference frame, and the ridge count between each pair of vertices. The problems with their approach

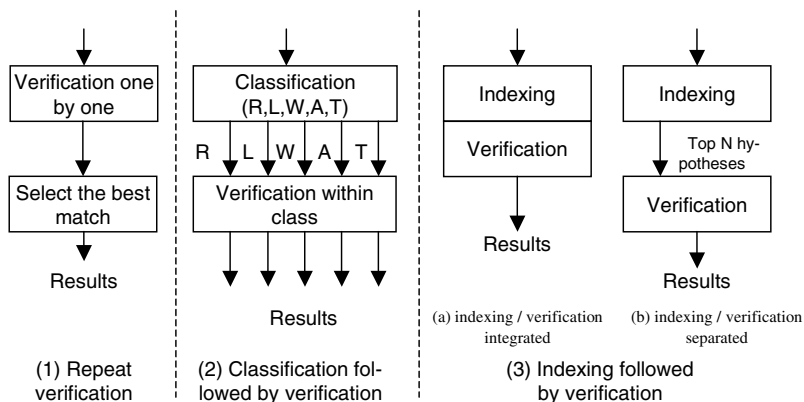


Fig. 2. Block diagram of three kinds of approaches to solve identification problem.

are: (a) the length changes are not insignificant under scale and shear; (b) the ridge angles change greatly with different quality images of the same finger; and (c) uncertainty of minutiae locations is not modeled explicitly. As a result, large size bins have to be used to handle distortions, which increases the probability of collisions and degrades the performance of their algorithm.

Our approach presented in this paper follows Germain et al. (1997) in that we also use the triplets of minutiae and ridge counts. However, the indexing and verification in our approach are separated (Fig. 2(b)). Firstly, we apply indexing techniques to find top  $N$  ( $N = 10\%$  in our experiments) hypotheses, and then apply verification technique to verify hypotheses. Furthermore, most features that we use are quite different from theirs. The features that we use are: triangle's angles, orientation, direction, maximum side, minutiae density and ridge counts. And we also use the constraints of the transformation to eliminate the

false corresponding triangles. Fig. 3 shows the block diagram of our approach. Minutiae are extracted by using a learned template based approach introduced by Bhanu and Tan (2001b). During the offline processing, template fingerprints are processed to construct the model database. During the online processing, features of the query fingerprint based on the triplets of minutiae are used to find the potential corresponding triangles. Then, top 10% hypotheses are generated according to the number of potential corresponding triangles. The transformation between each pair of potential corresponding triangles is estimated using mean square error. Finally, the constraints of the transformation are applied to eliminate the false corresponding triangles. The identification score is computed based on the number of corresponding triangles.

The contribution of this paper is that we develop a robust fingerprint identification approach, which can tolerate highly nonlinear deformations.

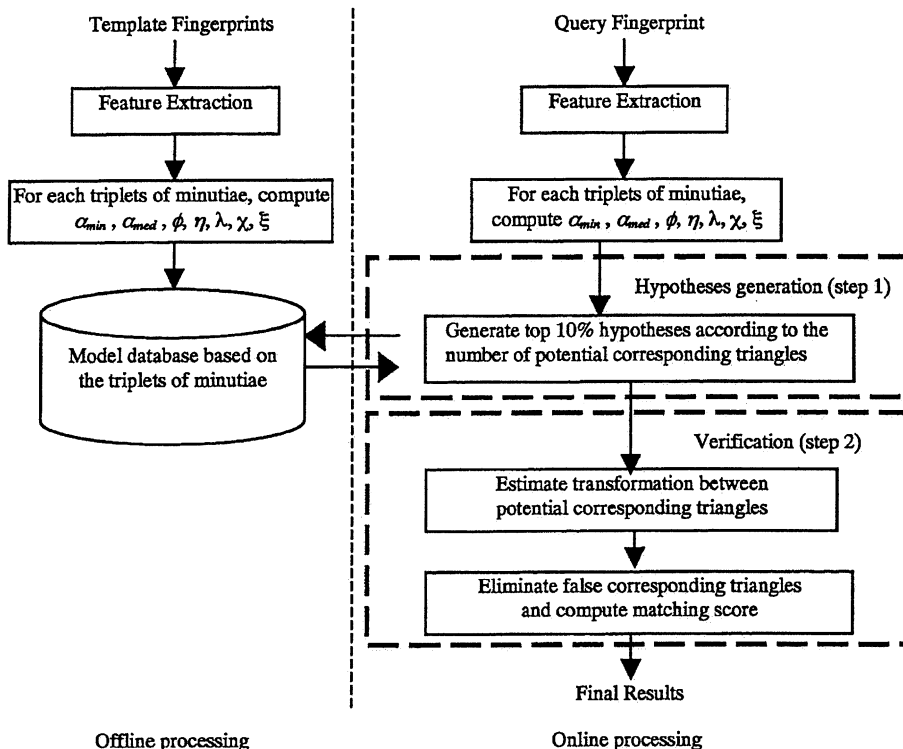


Fig. 3. Two step approach for fingerprint identification.

The performance of our approach on the NIST-4 database, which has a large portion of fingerprints of poor quality, shows that our approach is promising.

## 2. Technical approach

### 2.1. Find potential corresponding triangles

Fig. 4 shows a triangle. Without loss of generality, we assume that one vertex,  $O$ , of the triangle is  $(0, 0)$ , and it does not change under distortions. Since distance is invariant under translation and rotation and relatively invariant under scale, and angles are defined in terms of the ratio of distance, it can be proved that angles are invariant under these transformations. However, in fingerprint recognition, because of the uncertainty of minutiae locations, which is associated with feature extraction and shear, the location of each minutia translates in a small local area randomly and independently. Suppose the locations of points  $A$  and  $B$  are  $(x_1, 0)$  and  $(x_2, y_2)$ ,  $x_1 > 0$ ,  $y_2 > 0$  and  $x_2 \in (-\infty, +\infty)$ . Because of the uncertainty of minutiae locations,  $A$  and  $B$  move to  $A'(x_1 + \Delta x_1, 0)$  and  $B'(x_2 + \Delta x_2, y_2 + \Delta y_2)$ , respectively, and  $\alpha$  changes to  $\alpha + \Delta\alpha$ . Then

$$\tan \Delta\alpha = \frac{(x_1 - x_2)\Delta y_2 - y_2(\Delta x_1 - \Delta x_2)}{(x_1 - x_2)^2 + (x_1 - x_2)(\Delta x_1 - \Delta x_2) + y_2^2 + y_2\Delta y_2} \quad (1)$$

Suppose  $\Delta x_1$ ,  $\Delta x_2$  and  $\Delta y_2$  are independent, and  $-6 \leq \Delta x_i, \Delta y_2 \leq 6$ ,  $i = 1, 2$  and  $\Delta x_i$  and  $\Delta y_2$  are all integers, then

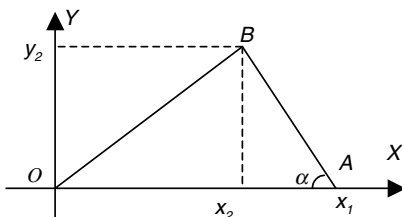


Fig. 4. Illustration of variables.

$$g(x_1, x_2, y_2) = E\{\Delta\alpha\} \approx \sum_{\Delta x_1=-6}^6 \sum_{\Delta x_2=-6}^6 \sum_{\Delta y_2=-6}^6 (|\tan \Delta\alpha| \times p(\Delta x_1)p(\Delta x_2)p(\Delta y_2)) \quad (2)$$

Suppose  $p(\Delta x_1)$ ,  $p(\Delta x_2)$  and  $p(\Delta y_2)$  are discrete uniform distributions in  $[-6, +6]$ . Let  $0 < x_1, y_2, |x_2| < L$ , where  $L$  is the maximum value of these variables in the image (in our experiments  $L = 300$ ). We compute  $g(x_1, x_2, y_2)$  at each point  $(x_1, x_2, y_2)$  based on whether  $\alpha$  is the minimum, median or maximum angle in the triangle. Notice that, if  $\alpha_{\min} < \delta_\alpha$  or  $\tau < \delta_\tau$ , then the uncertainty of minutiae locations may have more effect on  $\alpha_{\min}$  and  $\alpha_{\text{med}}$ , so we do not use these triangles in the model-base, where  $\tau$  is the minimum length of the sides in a triangle. Thresholds are  $\delta_\alpha = 10^\circ$ ,  $\delta_\tau = 20$ .

From Table 1, we observe: (1) the minimum and the median angles  $\alpha_{\min}$  and  $\alpha_{\text{med}}$  are more robust than the maximum angle  $\alpha_{\max}$  and they can be used to find the correspondences; (2)  $2^\circ$  can accommodate the uncertainty of most distortions and keep the size of the search space as small as possible. Using other distributions for  $p(\Delta x_1)$ ,  $p(\Delta x_2)$  and  $p(\Delta y_2)$ , we find the results similar to that in Table 1. More details of the analysis can be found in (Bhanu and Tan, 2001a).

The features we use to find potential corresponding triangles are defined as:

- *Angles  $\alpha_{\min}$  and  $\alpha_{\text{med}}$ :* Suppose  $\alpha_i$  are three angles in the triangle,  $i = 1, 2, 3$ . Let  $\alpha_{\max} = \max\{\alpha_i\}$ ,  $\alpha_{\min} = \min\{\alpha_i\}$ ,  $\alpha_{\text{med}} = 180^\circ - \alpha_{\max} - \alpha_{\min}$ , then the label of the triplets in this triangle is: if the minutia is the vertex of angle  $\alpha_{\max}$ , we label this point as  $P_i$ ; if the minutia is the vertex of angle

Table 1  
Percentage of the expectation of changes of angles less than the threshold

Angle's type	Angle change threshold					
	1°	2°	3°	4°	5°	6°
$\alpha_{\min}$	75.8	97.1	99.2	99.7	99.9	100.0
$\alpha_{\text{med}}$	74.4	92.4	97.0	98.6	99.3	99.6
$\alpha_{\max}$	32.1	82.8	93.6	97.1	98.6	99.2

$\alpha_{\min}$ , we label it as  $P_2$ ; the last minutia is labeled as  $P_3$ .

• *Triangle orientation  $\phi$* : Let  $Z_i = x_i + jy_i$  be the complex number ( $j = \sqrt{-1}$ ) corresponding to the coordinates  $(x_i, y_i)$  of point  $P_i$ ,  $i = 1, 2, 3$ . Define  $Z_{21} = Z_2 - Z_1$ ,  $Z_{32} = Z_3 - Z_2$  and  $Z_{13} = Z_1 - Z_3$ . Let  $\phi = \text{sign}(Z_{21} \times Z_{32})$ , where  $\text{sign}$  is the signum function and  $\times$  is the cross product of two complex numbers.

• *Triangle direction  $\eta$* : Search the minutia from top to bottom and left to right in the fingerprint, if the minutia is the start point of a ridge or valley, then  $v = 1$ , else  $v = 0$ .  $\eta$  is the combination of  $v_i$ ,  $v_i$  is the  $v$  value of point  $P_i$ ,  $i = 1, 2, 3$ .

• *Maximum side  $\lambda$* : Let  $\lambda = \max\{L_i\}$ , where  $L_1 = |Z_{21}|$ ,  $L_2 = |Z_{32}|$  and  $L_3 = |Z_{13}|$ .

• *Minutiae density  $\chi$* : In a local area ( $32 \times 32$  pixels) centered at the minutiae  $P_i$ , if there exists  $n_\chi$  minutiae, then minutiae density  $\chi_i = n_\chi$ .  $\chi$  is a vector consisting of all  $\chi_i$ 's.

• *Ridge counts  $\xi$* :  $\xi_1$  is the ridge count of the side  $P_1P_2$ ,  $\xi_2$  is the ridge count of the side  $P_2P_3$ , and  $\xi_3$  is the ridge count of the side  $P_3P_1$ .  $\xi$  is a vector consisting of all  $\xi_i$ 's.

If two triangles from two different fingerprints have the same feature values, then they are potential corresponding triangles.

In our implementation, we use a 7D array to represent the index space. Each element in the array is a vector that contains the information about triangles that are associated with the index. And all this information is computed during the offline processing.

### 2.2. Verify corresponding triangles

Suppose the sets of minutiae in the template and the query fingerprints are  $\{(t_{m,1}, t_{m,2})\}$  and  $\{(q_{n,1}, q_{n,2})\}$  respectively, where  $m = 1, 2, 3, \dots, M$ ,  $n = 1, 2, 3, \dots, N$ ,  $M$  and  $N$  are the number of minutiae in the template and the query fingerprints respectively. Let  $\Delta_t$  and  $\Delta_q$  be two potential corresponding triangles in the template and the query fingerprints, respectively. The coordinates of the vertices of  $\Delta_t$  and  $\Delta_q$  are  $(x_{i,1}, x_{i,2})$  and  $(y_{i,1}, y_{i,2})$ , respectively, and  $i = 1, 2, 3$ . Suppose  $X_i = [x_{i,1}, x_{i,2}]'$ ,  $Y_i = [y_{i,1}, y_{i,2}]'$ , and the transformation  $Y_i = F(X_i)$  between  $X_i$  and  $Y_i$  can be expressed as

$$Y_i = \begin{bmatrix} 1 & \delta h_x \\ \delta h_y & 1 \end{bmatrix} \begin{bmatrix} 1 + \delta s_x & 0 \\ 0 & 1 + \delta s_y \end{bmatrix} R \cdot X_i + T \quad (3)$$

where  $(\delta h_x, \delta h_y)$  and  $(1 + \delta s_x, 1 + \delta s_y)$  are the shear and scale parameters;

$$R = \begin{bmatrix} \cos \theta & -\sin \theta \\ \sin \theta & \cos \theta \end{bmatrix}$$

$\theta$  is the angle of rotation between two fingerprints; and  $T = [t_1, t_2]'$  is the vector of translation.

Since  $\delta h_x \ll 1$ ,  $\delta h_y \ll 1$  and  $\delta s_x \approx \delta s_y$ , we can simplify Eq. (2) to

$$Y_i = s \cdot R \cdot X_i + T \quad (4)$$

where  $s$  is the scaling factor.

We can estimate the transformation parameters by minimizing the sum of the squared distances between the transformed query points and their corresponding template points. That is,

$$\text{error} = \arg \min_{(s, \hat{R}, \hat{T})} \{\varepsilon^2\} \quad (5)$$

where  $\varepsilon^2 = \sum_{i=1}^3 \|Y_i - (\hat{s} \cdot \hat{R} \cdot X_i + \hat{T})\|^2$ ,  $\|V\|$  is the  $L_2$  norm of vector  $V$ .

The solution of Eq. (5) is

$$\begin{aligned} \hat{\theta} &= \arctan\left(\frac{B}{A}\right), \\ \hat{s} &= \frac{\sum_{i=1}^3 \{(X_i - \bar{X})' \hat{R}' (Y_i - \bar{Y})\}}{\sum_{i=1}^3 \{(X_i - \bar{X})' (Y_i - \bar{Y})\}}, \\ \hat{T} &= \bar{Y} - \hat{s} \cdot \hat{R} \cdot \bar{X} \end{aligned} \quad (6)$$

where

$$A = \sum_{i=1}^3 \{(\bar{x}_1 - x_{i,1})(y_{i,1} - \bar{y}_1) + (\bar{x}_2 - x_{i,2})(y_{i,2} - \bar{y}_2)\}$$

$$B = \sum_{i=1}^3 \{(\bar{x}_1 - x_{i,1})(y_{i,2} - \bar{y}_2) - (\bar{x}_2 - x_{i,2})(y_{i,1} - \bar{y}_1)\}$$

$$\bar{X} = \begin{bmatrix} \bar{x}_1 \\ \bar{x}_2 \end{bmatrix} = \sum_{i=1}^3 \bar{X}_i, \quad \bar{Y} = \begin{bmatrix} \bar{y}_1 \\ \bar{y}_2 \end{bmatrix} = \sum_{i=1}^3 \bar{Y}_i,$$

$$\hat{R} = \begin{bmatrix} \cos \hat{\theta} & -\sin \hat{\theta} \\ \sin \hat{\theta} & \cos \hat{\theta} \end{bmatrix}, \quad \hat{T} = \begin{bmatrix} \hat{t}_1 \\ \hat{t}_2 \end{bmatrix}. \quad (7)$$

If  $\hat{s}$ ,  $\hat{\theta}$ ,  $\hat{t}_1$  and  $\hat{t}_2$  are less than certain thresholds, then we take them as the parameters of the transformation between two potential corresponding triangles  $\Delta_t$  and  $\Delta_q$ . Otherwise, they are false correspondences. Based on the transformation  $\hat{F}(\hat{s}, \hat{\theta}, \hat{t}_1, \hat{t}_2) \forall j, j = 1, 2, 3, \dots, M$ , we compute

$$d = \arg \min_k \left\{ \left| \hat{F} \left( \begin{bmatrix} t_{j,1} \\ t_{j,2} \end{bmatrix} \right) - \begin{bmatrix} q_{k,1} \\ q_{k,2} \end{bmatrix} \right| \right\} \quad (8)$$

If  $d$  is less than a threshold  $T_d$ , then we define the points  $[t_{j,1}, t_{j,2}]'$  and  $[q_{k,1}, q_{k,2}]'$  are corresponding points. If the number of corresponding points based on  $\hat{F}(\hat{s}, \hat{\theta}, \hat{t}_1, \hat{t}_2)$  is greater than a threshold  $T_n$ , then we define  $\Delta_t$  and  $\Delta_q$  as the *corresponding triangles* between the template and the query fingerprints.

The identification score is simply the number of corresponding triangles.

### 2.3. Probability of false corresponding triangles

Suppose: (a)  $S$  is the size of the index space; (b)  $f_k$  is the number of triangles in the model database for image  $I_k$ , and these triangles are uniformly distributed in the indexing space; (c)  $b$  is the search redundancy for each triangle in the query image; (d)  $v_k$  is the number of corresponding triangles between image  $I$  and  $I_k$ ; (e)  $f_i$  is the number of triangles for the query image; and (f)  $p_0$  and  $p_1$  be the probabilities to find a corresponding triangle in the indexing space for image  $I_k$  in a single search and redundant search, respectively (Lamdan and Wolfson, 1991). Then

$$p_1 = 1 - (1 - p_0)^b \quad \text{and} \quad p_0 = \frac{f_k}{S} \quad (9)$$

In our approach,  $S \gg f_k$ ,  $p_0$  is a small value. So,  $p_1 \approx bp_0$ . The value of  $v_k$  that is greater than a threshold  $T$  can be computed using the Binomial distribution with  $p_1$ ,

$$P\{v_k > T\} = \sum_{i>T} \binom{f_i}{i} p_1^i (1 - p_1)^{f_i - i} \quad (10)$$

Since  $p_1 \ll 1$ , and  $f_i$  is large, the Binomial distribution can be approximated by the Poisson distribution with  $\xi = f_i \times p_1$ . Hence  $P\{v_k > T\}$  can be approximated by

$$P\{v_k > T\} \approx 1 - e^{-\xi} \sum_{i=0}^T \frac{\xi^i}{i!} \quad (11)$$

In our approach, we use  $1^\circ$  as the bin size for angles  $\alpha_{\min}$  and  $\alpha_{\text{med}}$ , and we search the corresponding triangles with the uncertainty of  $\pm 2^\circ$ . Hence,  $S = 207360000$ ,  $b = 9$ , if  $f_k = f_i \approx 11407$ , then we have  $p_0 = 5.501 \times 10^{-5}$ ,  $p_1 \approx 4.951 \times 10^{-4}$ ,  $\xi \approx 5.648$ . Fig. 5 shows the curve of  $P\{v_k > T\}$  with respect to  $T$ .

From Fig. 5, we observe that  $P\{v_k > T\}$  decreases quickly with respect to  $T$ . When  $T = 15$ ,  $P\{v_k > T\} = 0.0003$ . That is, if there is no fingerprint in the database corresponding to the query fingerprint, then the probability of finding 15 corresponding triangles between the query fingerprint and any fingerprints in the database is about 0.0003. We can use  $T = 15$  as the threshold to reject a query fingerprint which has no corresponding fingerprint in the database.

From Fig. 5, we observe that  $P\{v_k > T\}$  decreases quickly with respect to  $T$ . When  $T = 15$ ,  $P\{v_k > T\} = 0.0003$ . That is, if there is no fingerprint in the database corresponding to the query fingerprint, then the probability of finding 15 corresponding triangles between the query fingerprint and any fingerprints in the database is about 0.0003. We can use  $T = 15$  as the threshold to reject a query fingerprint which has no corresponding fingerprint in the database.

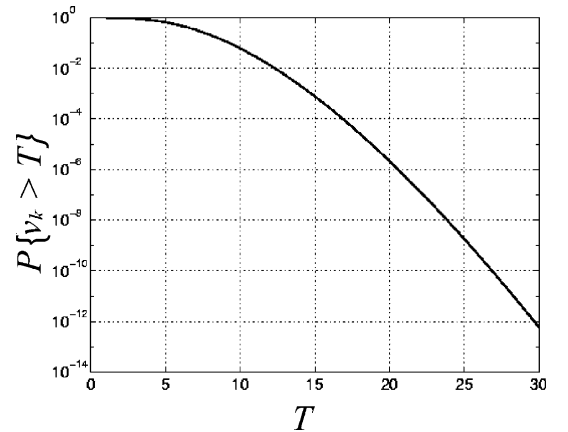


Fig. 5.  $P\{v_k > T\}$  with respect to  $T$ .

### 3. Experimental results

The database we use is the NIST Special Database 4 (NIST-4) (Watson and Wilson, 1992), which is a publicly available fingerprint database. Since the fingerprints in NIST-4 are collected by ink-based method, a large portion of fingerprints are of poor quality and contains certain other objects, such as characters and handwritten lines. The size of the fingerprint images is  $480 \times 512$  pixels with the resolution of 500 DPI.

NIST-4 contains 2000 pairs of fingerprints. Each pair is a different impression of the same finger. One pair of fingerprints is shown in Fig. 6. In our experiments, the first 2000 fingerprints (f0001\_01–f2000\_10) are used to construct the model database, and the second 2000 fingerprints (s0001\_01–s2000\_10) are used as the query fingerprints. Conceptually, we did 2000 queries to find the genuine acceptance rate (GAR) and 3 998 000 queries ( $2000 \times 1999$ ) queries to find the false acceptance rate (FAR). The parameters that we use are shown in Table 2. The receiver operating characteristic (ROC) curve is defined as the plot of GAR against FAR. Fig. 7 shows the ROC curve of the proposed approach on NIST-4.

From Fig. 7, we observe that without rejecting any fingerprints from NIST-4 database, the GAR and FAR can reach 83.0% and 0.2%, respectively. As the threshold for identification score increases, the FAR decreases to 0.0011% while the GAR is 71.8%. To the best of our knowledge, this is the first paper, which shows the identification results obtained automatically by computer program on the entire NIST-4 database.

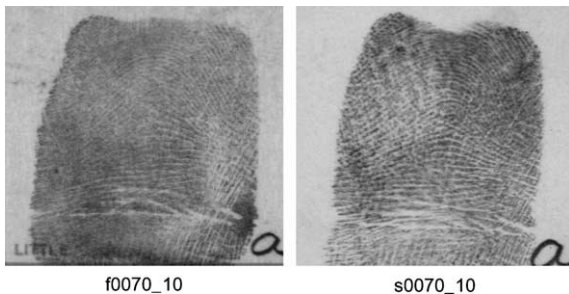


Fig. 6. Sample images in NIST-4 database.

Table 2  
Parameter used in experiments

Parameters	Value
$T_s$ , threshold to constrain scaling factor $\hat{s}$	$0.85 < \hat{s} < 1.15$
$T_\theta$ , threshold to constrain rotation angle $\hat{\theta}$	$-30^\circ < \hat{\theta} < 30^\circ$
$T_1$ and $T_2$ , threshold to constrain translations $\hat{t}_1$ and $\hat{t}_2$	$ \hat{t}_1  < 150$ $ \hat{t}_2  < 100$
$T_d$ , threshold to find the corresponding points	$T_d = 12$ pixels
$T_n$ , threshold to find the corresponding triangles	$T_n = 8$

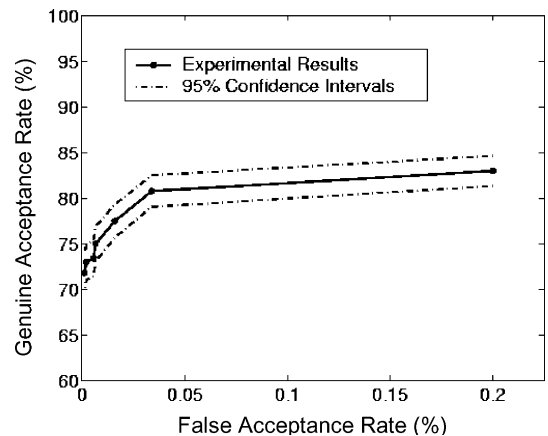


Fig. 7. ROC curve of the experimental results.

Results on NIST-4 are reported in (Kovacs-Vajna, 2000). However, the approach in (Kovacs-Vajna, 2000) is for verification only and 6.0% data are rejected *manually* by the author because of bad quality. Without dynamic time warping (DTW) for the detailed verification, the FAR is 10.0%, which is unacceptable, although the GAR is 85.0%. It makes no sense for us to compare the performance reported in (Kovacs-Vajna, 2000) with DTW since the author has not used the entire database, and we do not know which of the fingerprints have been rejected manually. We also implemented the approach as described in (Germain et al., 1997), and Fig. 8 shows the correct indexing power (CIP) (Bhanu and Tan, 2001a) of the approach in (Germain et al., 1997), where CIP is defined as the percentage of the correctly indexed images. If we take the top 1 hypothesis as the identification result, then GAR is 53.0% while

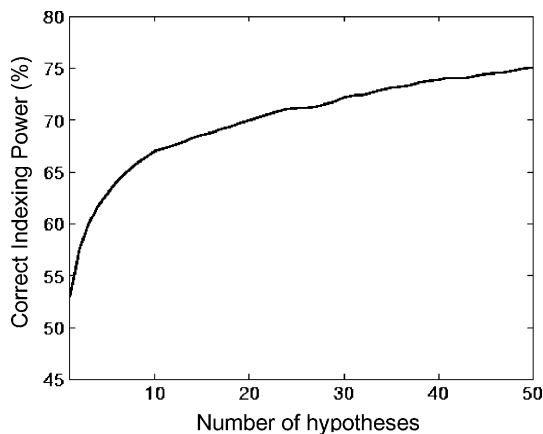


Fig. 8. CIP of the approach (Germain et al., 1997) on NIST-4.

FAR is greater than 10.0%. This performance on NIST-4 database is not good. One important reason is that the approach in (Germain et al., 1997) does not take into account the scale distortion, which is obviously present in NIST-4 database.

Examining the experimental results, we find that: (a) the zero identification scores for most genuine queries are due to the poor quality of fingerprints. There are not enough overlapped areas from which the feature extraction procedure can extract enough corresponding minutiae; (b) the nonzero identification scores for most imposter queries are due to the highly similar structures in two different fingerprints.

#### 4. Conclusions

In this paper, we proposed a fingerprint identification approach based on the triplets of minutiae. The features we use to find potential corresponding triangles are based on the triplets of minutiae and can tolerate reasonable distortions, including translation, rotation, scale, shear, local perturbation, occlusion and clutter. Constraints for translation, rotation and scale are applied to the transformation parameters to eliminate the false corresponding triangles. The number of corresponding triangles provides a good local method

to measure the similarities between two fingerprints. Since we only take into account the top 10% hypotheses in the verification step, it provides a reduction by a factor of 10 for the number of the hypotheses that need to be considered if linear search is used. We achieve promising experimental results on the NIST-4 database, which has a large portion of poor quality fingerprints.

#### References

- Bhanu, B., Tan, X., 2001a. A triplet based approach for indexing of fingerprint database for identification. In: Proc. Internat. Conf. on Audio- and Video-Based Biometric Person Authentication, pp. 205–210.
- Bhanu, B., Tan, X., 2001b. Learned templates for feature extraction in fingerprint images. In: Proc. IEEE Conf. on Computer Vision and Pattern Recognition, vol. 2, pp. 591–596.
- Cappelli, R., Lumini, A., Maio, D., Maltoni, D., 1999. Fingerprint classification by directional image partitioning. *IEEE Trans. PAMI* 21 (5), 402–421.
- Germain, R.S., Califano, A., Colville, S., 1997. Fingerprint matching using transformation parameter clustering. *IEEE Comput. Sci. Eng.* 4 (4), 42–49.
- Jain, A.K., Hong, L., Pankanti, S., Bolle, R., 1997. An identity-authentication system using fingerprints. *Proc. IEEE* 85 (9), 1364–1388.
- Jain, A.K., Prabhakar, S., Hong, L., 1999. A multichannel approach to fingerprint classification. *IEEE Trans. PAMI* 21 (4), 348–359.
- Jiang, X., Yau, W.Y., 2000. Fingerprint minutiae matching based on the local and global structures. In: Proc. Internat. Conf. on Pattern Recognition, pp. 1038–1041.
- Kovacs-Vajna, Z.M., 2000. A fingerprint verification system based on triangular matching and dynamic time warping. *IEEE Trans. PAMI* 22 (11), 1266–1276.
- Lamdan, Y., Wolfson, H.J., 1991. On the error analysis of ‘Geometric Hashing’. In: Proc. Internat. Conf. on Computer Vision and Pattern Recognition, pp. 22–27.
- Marcialis, G.L., Roli, F., Frasconi, P., 2001. Fingerprint classification by combination of flat and structure approaches. In: Proc. AVBPA, pp. 241–246.
- Wilson, C.L., Candela, G.T., Watson, C.I., 1993. Neural network fingerprint classification. *J. Artif. Neural Networks* 1 (2), 203–228.
- Watson, C.I., Wilson, C.L., 1992. NIST special database 4, fingerprint database, US National Institute of Standards and Technology.
- Yao, Y., Frasconi, P., Pontil, M., 2001. Fingerprint classification with combination of support vector machines. In: Proc. AVBPA, pp. 253–258.